JGR Earth Surface

RESEARCH ARTICLE
10.1029/2021JF006366

Secondary Minerals Drive Extreme Lithium Isotope Fractionation During Tropical Weathering

María Chapela Lara[1,2], Heather L. Buss[3], Michael J. Henehan[2], Jan A. Schuessler[2], and William H. McDowell[1]

[1]Department of Natural Resources and the Environment, University of New Hampshire, Durham, NH, USA, [2]GFZ German Research Centre for Geosciences, Section 3.3 Earth Surface Geochemistry, Potsdam, Germany, [3]School of Earth Sciences, University of Bristol, Bristol, UK

Key Points:

- Lowest δ^7Li values reported to date in nature (porewater = −27‰; bulk regolith = −38‰; exchangeable Lithium (Li) = −50‰)
- Large isotopic differences driven by clay precipitation, dissolution, and re-precipitation processes
- Li isotopes may not be appropriate tracers of weathering intensity for very highly weathered catchments

Supporting Information:

Supporting Information may be found in the online version of this article.

Correspondence to:

M. Chapela Lara,
glzmcl@my.bristol.ac.uk

Citation:

Chapela Lara, M., Buss, H. L., Henehan, M. J., Schuessler, J. A., & McDowell, W. H. (2022). Secondary minerals drive extreme lithium isotope fractionation during tropical weathering. *Journal of Geophysical Research: Earth Surface*, *127*, e2021JF006366. https://doi.org/10.1029/2021JF006366

Received 28 JUL 2021
Accepted 31 JAN 2022

Abstract Lithium isotopes are used to trace weathering intensity, but little is known about the processes that fractionate them in highly weathered settings, where secondary minerals play a dominant role in weathering reactions. To help fill this gap in our knowledge of Li isotope systematics, we investigated Li isotope fractionation at an andesitic catchment in Puerto Rico, where the highest rates of silicate weathering on Earth have been documented. We found the lowest δ^7Li values published to date for porewater (−27‰) and bulk regolith (−38‰), representing apparent fractionations relative to parent rock of −31‰ and −42‰, respectively. We also found δ^7Li values that are lower in the exchangeable fraction than in the bulk regolith or porewater, the opposite than expected from secondary mineral precipitation. We interpret these large isotopic offsets and the unusual relationships between Li pools as resulting from two distinct weathering processes at different depths in the regolith. At the bedrock-regolith transition (9.3–8.5 m depth), secondary mineral precipitation preferentially retains the lighter ^{6}Li isotope. These minerals then dissolve further up the profile, leaching ^{6}Li from the bulk solid, with a total variation of about +50‰ *within* the profile, attributable primarily to clay dissolution. Importantly, streamwater δ^7Li (about +35‰) is divorced entirely from these regolith weathering processes, instead reflecting deeper weathering reactions (>9.3 m). Our work thus shows that the δ^7Li of waters draining highly weathered catchments may reflect bedrock mineralogy and hydrology, rather than weathering intensity in the regolith covering the catchment.

Plain Language Summary Weathering is the process by which rocks are altered at the Earth's surface, transforming fresh minerals into clays with some loss of chemical elements to rivers and eventually oceans. Understanding how intense weathering is now, and has been in the past, is important because it supplies nutrients for ecosystems and is part of the Earth's long-term carbon cycle (and thus, climate regulation). To do this, geochemists have developed tracers of weathering intensity, of which Li isotopes (expressed as δ^7Li) are considered to be the best. However, we know little about the behavior of Li isotopes in the tropics, where weathering is the most intense. To help make δ^7Li a more robust tracer, we sampled a 10 m deep soil profile at a tropical catchment in Puerto Rico where rocks are dissolving very fast. We found that weathering here is so intense that clays are continuously dissolving, producing the lowest δ^7Li values ever recorded on Earth, but that the stream water draining the catchment does not reflect these values. Our work thus expands the range of known values of this tracer and warns geochemists that δ^7Li in rivers might not be directly related to weathering intensity in tropical catchments.

1. Introduction

Lithium (Li) isotopes are considered one of the best tracers of silicate weathering (past and present) because they are relatively insensitive to confounding processes such as carbonate formation/dissolution or biological cycling (see overviews by Penniston-Dorland et al., 2017 and Pogge von Strandmann et al., 2020). Instead, the fractionation of Li isotopes during weathering can be mainly attributed to secondary minerals preferentially taking up the lighter isotope, ^{6}Li (Hindshaw et al., 2019; Pistiner & Henderson, 2003; Verney-Carron et al., 2011; Vigier et al., 2008; Wimpenny et al., 2015). As a result of this isotopic fractionation during secondary mineral formation, the Li isotope signature of weathering products can be broadly related to the degree of weathering (also known as weathering intensity). When primary minerals are still predominant in the regolith (here defined as all weathered material overlying cohesive bedrock), Li isotopes are not strongly fractionated relative to the bedrock (Huh et al., 2004; Lemarchand et al., 2010; Pogge von Strandmann et al., 2012; Ryu et al., 2014) but at more advanced

weathering stages, where secondary minerals dominate, bulk regolith shows δ^7Li values increasingly lower than its parent rock (Clergue et al., 2015; Huh et al., 2004; Kisakűrek et al., 2005; Liu et al., 2013; Rudnick et al., 2004; Ryu et al., 2014). Weathering also enriches waters in the heavy isotope, ^{7}Li, providing information about the balance of primary silicate dissolution relative to secondary mineral formation–i.e., weathering intensity–at the catchment level (Dellinger et al., 2015; Millot et al., 2010; Misra & Froelich, 2012; Pogge von Strandmann et al., 2006; Vigier et al., 2009).

The utility of Li isotopes as a weathering proxy thus depends on understanding the reactions that fractionate them across a wide range of environmental settings. However, most of what we know about Li isotope fractionation in the critical zone comes from studies of temperate sites. Likewise, most laboratory experiments have addressed the dissolution of primary minerals and the precipitation of clays, but relatively little is known about the potential Li isotopic fractionation exerted by other secondary minerals typical of advanced weathering stages (like Fe, Al, and Mn oxides) or by weathering processes after secondary minerals have precipitated, such as changes in crystallinity (ripening), desorption, and dissolution of secondary and refractory minerals. Therefore, to better establish Li isotopes as a robust tracer of weathering intensity, a more complete understanding of the processes that control their fractionation at late weathering stages is needed.

To this end, we investigated the Li isotope systematics of a well-studied weathering profile at the catchment with the fastest documented silicate weathering rates on Earth (~334 mm y^{-1}; Dosseto et al., 2012), which is covered by tens of meters of highly leached regolith comprised only of secondary minerals and primary quartz (Buss et al., 2013; Dosseto et al., 2012). Laboratory studies would predict that such abundant secondary mineral formation should drive significant Li isotope fractionation. On the other hand, the stream chemistry of other elements measured at this site appears to be set by weathering reactions occurring below the bedrock-regolith interface (Chapela Lara et al., 2017; Yi-Balan et al., 2014). This site, therefore, offers a unique opportunity to test the relative importance of regolith versus bedrock weathering processes in setting the δ^7Li of waters draining highly weathered tropical catchments.

2. Materials and Methods

2.1. Regolith Profile

The regolith profile we studied is located on a ridgetop within the andesitic volcaniclastic Bisley 1 catchment, part of the Luquillo Critical Zone Observatory in NE Puerto Rico (Figure S1 in Supporting Information S1). This site is covered by a mature montane tropical forest with a mean annual precipitation of 3,878 mm and a mean daily temperature of 24.2°C (Gioda et al., 2013).

The regolith at this site (0–8.5 m depth) is highly weathered (Chemical Index of Alteration [CIA] >98%; Table 1; Figure S2a in Supporting Information S1) and almost completely depleted of base cations (e.g., 90% loss of Ca and 100% loss of Na; Chapela Lara et al., 2018). The mineralogy of this regolith also reflects a high degree of weathering: about 74 wt. % kaolinite, 15 wt. % illite, 5 wt. % Fe(III)-(hydr)oxides, and 20 wt. % quartz (Buss et al., 2017; Figure S2c and Table S1 in Supporting Information S1). At the bedrock-regolith transition (9.3–8.5 m depth), only chlorite (10 wt. %) and orthoclase (3 wt. %) remain of the parent rock mineral assemblage (plagioclase, chlorite, quartz, pyroxene, amphibole, epidote, prehnite; Buss et al., 2013).

Saharan dust contributes notable amounts of several elements to the shallow regolith (~0–1.8 m depth) in the Luquillo Mountains, including P (McClintock et al., 2015; Pett-Ridge, 2009), Mg (Chapela Lara et al., 2017), Mn, and Y (Chapela Lara et al., 2018). Input of Li from Saharan dust has also been documented in the Caribbean region (δ^7Li = +0.70‰, [Li] = 2.4–2.9 mmol kg^{-1}; Clergue et al., 2015).

2.2. Sample Collection and Elemental Analyses

Regolith samples were collected approximately every 30–60 cm depth by hand-augering until auger refusal at 9.3 m depth. Each solid regolith sample was homogenized, dried at 40°C and sieved to <2 mm. To estimate the proportion of major and trace elements held in the regolith exchange complex, an extraction with 0.1 M NH_4-acetate was performed (for further details, see Buss et al., 2017). Porewater was sampled from several depths at the same site in November 2009, using nested suction lysimeters installed by the USGS in 2007 (Buss et al., 2017).

Table 1
Li Concentrations and Lithium Isotopic Composition of Bulk Regolith, Bedrock, and Vegetation

Sample	Depth m	Li μg g^{-1}	Li mM kg^{-1}	Nb μg g^{-1}	Cs μg g^{-1}	CIA[a] %	$\tau_{Li,Nb}$[b]	δ^7Li ‰	2SD[d] ‰	n[d]
Bulk regolith										
B1S1-0	0.0	10.4	1.5	2.2	0.5	99.2	−0.65			
B1S1-31	0.3	10.0	1.4	2.7	0.7	99.3	−0.73			
B1S1-61	0.6	8.1	1.2	4.4	0.4	99.5	−0.86	10.90	0.19	3
B1S1-91	0.9	6.0	0.9	2.8	0.3	99.5	−0.84	9.27	0.20	3
B1S1-122	1.2	7.1	1.0	8.5	0.3	99.6	−0.94	7.37	0.18	3
B1S1-152	1.5	6.9	1.0	2.4	0.2	99.7	−0.79	8.33	0.12	3
B1S1-183	1.8	8.3	1.2	2.4	0.3	99.7	−0.74	12.60	0.42	2
B1S1-183*								12.72	0.01	3
B1S1-274	2.7	9.0	1.3	2.4	0.4	99.3	−0.72	8.62	0.17	3
B1S1-427	4.3	10.1	1.5	2.0	0.4	99.3	−0.63	2.17	0.21	3
B1S1-549	5.5	7.5	1.1			99.5		−5.19	0.16	3
B1S1-640	6.4	15.0	2.2	1.6	0.7	99.2	−0.29	−12.33	0.24	3
B1S1-640*								−12.53	0.15	3
B1S1-701	7.0	14.5	2.1			98.7		−18.15	0.07	3
B1S1-762	7.6	10.5	1.5			98.4		−18.87	0.27	3
B1S1-853	8.5					98.7				
B1S1-823	8.2	21.3	3.1	2.0	0.9	99.2	−0.20	−20.83	0.15	3
B1S1-899	9.0	43.1	6.2			97.4		−37.83	0.25	3
B1S1-899*								−37.84	0.09	3
B1S1-929	9.3	68.6	9.9	2.1	0.8	96.3	1.48	−36.97	0.28	3
B1S1-929*								−36.90	0.07	3
Drilled bedrock										
B1W2-1-2		13.8	2.0	1.1	0.05	48.25		4.20	0.25	3
B1W2-2-2		18.9	2.7			45.71		3.84	0.21	3
B1W2-6-2		18.2	2.6	1.3	0.35	50.03		4.21	0.17	3
B1W2-6-2*								4.40	0.40	3
B1W2-7-2[c]		20.0	2.9			73.90		10.93	0.28	3
B1W1-9-3[c]		40.0	5.8			82.30		6.29	0.27	3
Boulder B1P1		10.3	1.5	3.2	0.08	45.36		−0.01	0.13	3
Vegetation										
Tabonuco leaves		0.4	0.1					3.37	0.10	4
Reference materials										
OSIL Seawater								31.28	0.36	3
BHVO-2 basalt								4.55	0.51	4
BCR-2 basalt								2.94	0.14	1
SRM 2709a San Joaquin soil								−0.65	0.18	1

Note. * Full-procedure repeats.
[a]CIA = Chemical Index of Alteration (Equation S1 in Supporting Information S1) = $100[Al_2O_3/(Al_2O_3 + CaO^* + Na_2O + K_2O)]$. [b]$\tau_{Li,Nb}$ = mass transfer coefficient (Equation S2 and Text S1 in Supporting Information S1). [c]Slightly altered bedrock ("saprock" in Buss et al., 2013). [d]SD is the standard deviation within the same analytical session (n = number of repeats) for samples, BCR-2 and San Joaquin Soil and the standard deviation over different analytical sessions for OSIL and BHVO-2 (n = number of analytical sessions).

Table 2
Li and δ^7Li of Porewater and the Local Stream

Sample	Depth m	Li µg L^{-1}	Li µmol L^{-1}	δ^7Li ‰	2SD[a] ‰	n[a]
Porewater						
B1S1-0.5	0.2	0.57	0.08			
B1S1-1	0.3	0.91	0.13	7.94	0.30	3
B1S1-2	0.6	0.81	0.12	3.37	0.18	3
B1S1-3	0.9	0.71	0.10	5.91	0.23	3
B1S1-4	1.2	0.75	0.11	3.04	0.24	3
B1S1-5	1.5	1.04	0.15	−1.93	0.26	3
B1S1-6	1.8	0.69	0.10	−1.80	0.23	3
B1S1-14	4.3	3.25	0.47	−14.85	0.26	3
B1S1-30.5	9.3	7.86	1.13	−26.71	0.16	3
Stream water at low flow *						
Bisley 1–2010		0.24	0.035	32.00		1
Bisley 1–2012		0.27	0.039	36.67	0.32	2

Note. *Values corrected for small sample size are in Table S3 in Supporting Information S1.
[a]SD it the standard deviation within the same analytical session (n = number of repeats).

Table 3
Lithium and δ^7Li of the Regolith Exchangeable Fraction (NH_4-Acetate Extract)

Sample	Depth m	Li µM kg $regolith^{-1}$	δ^7Li* ‰	2SD[a] ‰	n[a]
B1S1-60-EC	0.6	2.51			
B1S1-180-EC	1.8	1.83			
B1S1-310-EC	3.1	4.03			
B1S1-427-EC	4.3	2.80			
B1S1-490-EC	4.9	2.36			
B1S1-549-EC	5.5	3.70	−19.78	0.22	3
B1S1-640-EC	6.4	3.18			
B1S1-701-EC	7.0	3.54	−39.03	0.79	3
B1S1-762-EC	7.6	5.95			
B1S1-823-EC	8.2	6.69	−44.38	0.65	3
B1S1-850-EC	8.5	14.28			
B1S1-899-EC	9.0	12.02	−49.63	0.52	3
B1S1-929-EC	9.3	20.28	−46.42	0.24	3

Note. *Values corrected for small sample size are in Table S3 in Supporting Information S1.
[a]SD is the standard deviation within the same analytical session (n = number of repeats).

Stream water samples were collected at low flow in July 2010 and July 2012 at the outlet of the catchment (Figure S1 in Supporting Information S1). All water samples were filtered to 0.45 µm (SFCA-membrane, Cole-Parmer) into acid-washed HDPE bottles following the USGS procedures at this site (e.g., Murphy & Stallard, 2012).

Three samples from drilled boreholes were chosen as representative of the mineralogy and chemical composition of the fresh bedrock, as well as a corestone sampled from the stream and two additional borehole samples with signs of incipient alteration, such as oxidation along fractures (Buss et al., 2013). Leaf material from the predominant tree species at the site (Tabonuco, *Dacryodes excelsa*) was also collected, oven-dried (≤60°C) and milled.

Major and trace elements in bulk regolith and bedrock samples were analyzed by SGS Laboratories (Toronto, Ontario, Canada) by ICP-AES after lithium metaborate fusion digestion (Buss et al., 2017) and some, including Li, were also analyzed at the USGS by ICP-MS after multi-acid digestion. The elemental composition of vegetation, porewater, and NH_4-acetate extracts was measured by ICP-MS after multi-acid digestion at Penn State University (vegetation) or the USGS (porewaters and NH_4-acetate extracts; Buss et al., 2017; Chapela Lara et al., 2017). Major elements in stream water were measured by ion chromatography at the University of New Hampshire (Table S3 in Supporting Information S1; McDowell et al., 2021c). To complement bulk regolith and bedrock data presented in Chapela Lara et al. (2018), further samples were measured for trace element composition at GFZ-Potsdam by ICP-OES (solids) or iCAP ICP-MS (exchangeable fraction and stream water; Tables 1–3).

For Li isotopic analysis, sub-samples of bulk regolith and rocks were digested on a hot plate at 110°C, using ultrapure concentrated HF and HNO_3. Subsequently, organic matter was oxidized sequentially with H_2O_2, aqua regia, and concentrated HNO_3 (more details in Schuessler et al., 2018). For water samples and NH_4-acetate extracts, the volume necessary to obtain ∼30 ng of Li was evaporated, treated with H_2O_2 + HNO_3 to remove organic matter and dried down again. Vegetation samples were treated repeatedly with concentrated HNO_3, H_2O_2, and aqua regia on a hotplate at 110°C, ultrasonicated and evaporated, until organic matter was fully removed. The residues from all types of samples were evaporated on a hotplate, treated again with H_2O_2 + HNO_3 to remove any remaining organic matter, and re-dissolved in 0.3 M HNO_3. An aliquot was taken for concentration measurements and the rest of the solution was dried down for isotope measurements.

2.3. Lithium Separation and Isotope Analyses

Lithium was separated from the matrix using a procedure based on previously established methods (e.g., Golla et al., 2021; Kisakürek et al., 2004; Zhang et al., 2021). Briefly, all samples were re-dissolved in 0.2 M HCl and loaded into 3 ml Bio-Rad AG 50W X12 (200–400 µm mesh) ion-exchange columns, using 0.2 M HCl as the eluent. The concentrations of Li and major elements of samples, blanks and standards were checked by iCAP ICP-MS after column separation, to ensure no Li contamination (typically 0.005 ng Li in the total process blanks and 0.003 ng Li in the column blanks) and a sum of matrix elements (Na, Ca, Mg, Zn, and Sr) lower than that of Li. The recovery of Li after purification was always 99.9% or higher, assuring negligible fractionation during the exchange chromatography. The purified samples were

evaporated, treated with H_2O_2 + HNO_3 to remove any organic leachates from the columns and re-dissolved in 0.3 M HNO_3 for isotopic measurements.

Lithium isotope analyses were performed at the Helmholtz Laboratory for the Geochemistry of the Earth Surface (HELGES), at GFZ-Potsdam, by MC-ICP-MS on a Thermo Neptune Plus. Samples were bracketed with the LSVEC standard with a concentration within ±10% of that of the sample. We express the Li isotopic ratios in common delta notation using LSVEC as the standard. The reference materials that were processed with each sample batch through the same procedures, yielded δ^7Li values of +31.3 ± 0.36‰ (2SD, n = 3) for OSIL seawater, +2.9 ± 0.25‰ (2SE, n = 1) for BCR-2 basalt, +4.55 ± 0.51‰ (2SD, n = 4) for BHVO-2 basalt, 0.18 ± 0.14‰ (2SE, n = 1) for JG-2 granite; and −0.65 ± 0.18‰ (2SE, n = 1) for SRM 2709a San Joaquin Soil (Table 1). These values are in good agreement with published long-term average δ^7Li values at the GFZ (San Joaquin Soil = −0.5 ± 0.2‰; Weynell et al., 2017, 2021) and with published δ^7Li values for these reference materials measured elsewhere by MC-ICP-MS: Atlantic Seawater = +31.3 ± 0.6 ‰ (Pogge von Strandmann, Schmidt, et al., 2019); BHVO-2 = +4.29 to +4.68 ‰; BCR-2 = +2.6 to +2.87 ‰ (Choi et al., 2013 and references therein). Additionally, in-house consistency standards ($LiNO_3$, Li_2CO_3, Baker + Merck; Weynell et al., 2017) were run with each analytical session to monitor accuracy and repeatability. Based on these analyses, for sample sizes of more than 20 ng Li, we estimate the overall uncertainty of the method to be 0.51‰.

For seven of our samples (exchangeable fraction and stream water; Tables 2 and 3, Table S2 in Supporting Information S1), insufficient Li was available to meet the minimum sample size of 20 ng Li for which the protocols for Li isotope measurement had been optimized at the HELGES laboratory. To ensure the accuracy of our measurements in this situation, we ran different quantities of OSIL seawater (1, 2, 3, 8, 12, 16, 20, and 100 ng Li) through the same protocol and found that our method–while reliable in reproducing reference material δ^7Li values within the 20–100 ng range of Li for which it was designed–systematically fractionated samples toward higher values below 20 ng Li (Figure S3 in Supporting Information S1). The magnitude of this effect increased with decreasing sample size, reaching up to 1.8‰ for samples of 1 ng Li (Figure S3 in Supporting Information S1). Extensive investigations revealed this offset was caused by preferential retention of a small fraction of ^{6}Li on resin that had degraded after storage in MilliQ water, similar to the effect observed by Kuessner et al. (2020) of progressively higher δ^7Li values when re-using resin more than three times. Although this resin-induced fractionation is very small relative to the magnitude of the isotopic variability observed in our samples (Figures 1d and 2), we devised a Monte Carlo-based correction for samples analyzed using less than 20 ng Li (Text S2, Table S2 in Supporting Information S1). The magnitude of this correction ranges from +0.6 to +1.8‰ and the total uncertainty (incorporating uncertainty in the analysis and correction) ranges from 0.5 to 0.8 ‰ (Table S2 in Supporting Information S1). We use the corrected values for these seven samples in all figures and the rest of the manuscript.

3. Results

Lithium concentrations [Li], increase with depth in all measured fractions. Bulk regolith [Li] increases from a minimum of 0.9 mmol kg^{-1} at 0.9 m depth to a maximum of 9.9 mmol kg^{-1} at 9.3 m depth (Figure 1a; Table 1). Exchangeable fraction (NH_4-acetate extract) [Li] increases from a minimum of 1.8 µmol kg^{-1} at 1.8 m depth to a maximum 20.3 µmol kg^{-1} at 9.3 m depth (Figure 1b). Porewater [Li] increases from a minimum of 0.1 µmol L^{-1} at 0.9 m depth to 1.3 µmol L^{-1} at 9.3 m depth (Figure 1c). The [Li] of the stream is ~37 nmol L^{-1} (Figure 1c; Table 2), which is low compared to large rivers globally (about 215 nmol L^{-1}; Huh et al., 1998) but similar to other tropical streams draining andesitic (~55 nmol L^{-1}; Fries et al., 2019) or basaltic lithologies (Henchiri et al., 2014; Huh et al., 2001, 2004).

Fresh bedrock δ^7Li values range between +3.8‰ and +4.4‰, typical of mafic to intermediate igneous rocks (Penniston-Dorland et al., 2017, and references therein). Rock samples showing signs of incipient weathering have δ^7Li values similar to, or slightly higher than, fresh bedrock (−0.01‰ to +10.9‰; Figure 1d; Table 1). Bulk regolith has δ^7Li values between −37.8‰ and +12.7‰, with a clear increasing trend from depth upwards (Figure 1d). However, above 1.5 m depth, a slight shift toward lower δ^7Li is seen in the bulk regolith (Figure 1d), consistent with the approximate depth of Saharan dust influence at this site (e.g., Chapela Lara et al., 2018).

Porewater δ^7Li also increases from depth toward the surface, from δ^7Li = −26.7‰ at 9.3 m depth to +7.9% at 0.3 m depth (Table 2; Figure 1d). Porewater is isotopically lighter than the bulk regolith for most of the profile, except in the two deepest samples (Figure 1d).

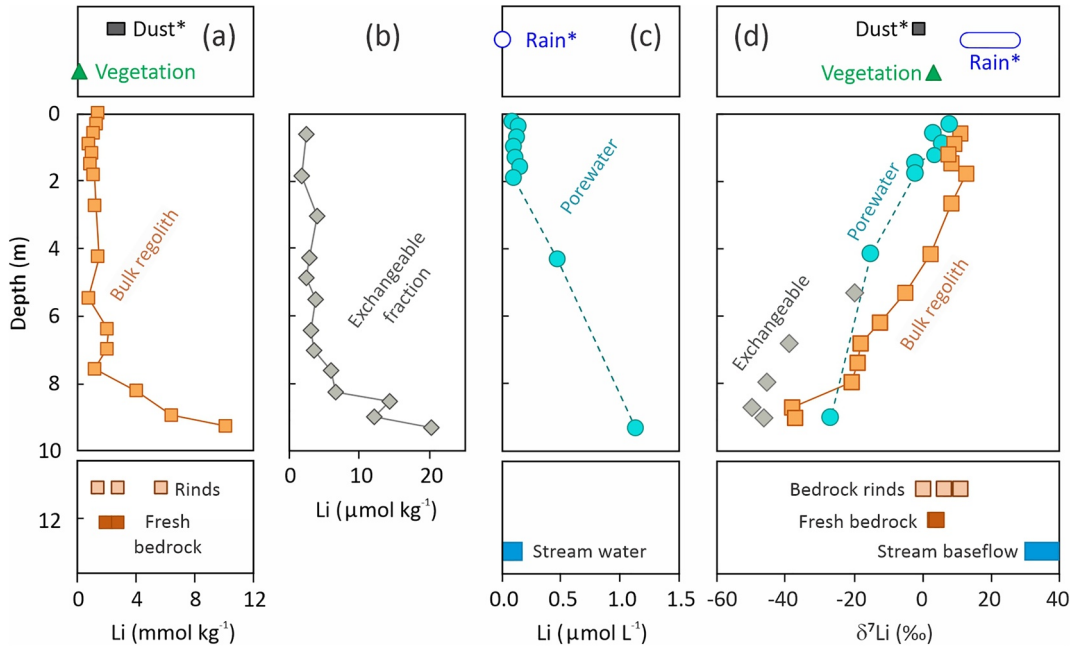

Figure 1. Variation of Lithium (Li) concentration with depth in (a) bulk solid, (b) the exchangeable fraction, and (c) porewater (note different concentration units in the *X*-axis). Li generally increases with depth in all three pools. (d) δ^7Li variation with depth in bulk regolith, porewater, and the exchangeable fraction. All three compartments show a generally increasing trend toward the surface of the profile. [Li] and δ^7Li values of fresh bedrock, slightly altered bedrock (rinds), vegetation, Saharan dust, rain, and stream water are given for reference (depth arbitrary). Measurement uncertainties (Tables 1–3, Table S2 in Supporting Information S1) are smaller than the symbols. *Li and δ^7Li values for Saharan dust and rain are from Clergue et al. (2015), collected in the Caribbean island of Guadeloupe (δ^7Li = −0.70‰; [Li] = 2.4–2.9 mmol kg^{-1}).

The δ^7Li values in the deepest samples of the profile are, to our knowledge, the lowest δ^7Li published to date for porewater (δ^7Li = −26.7 ‰) or bulk regolith (δ^7Li = −37.8 ‰; Figure 2). These values also represent the largest difference between a rock and its weathering products ($\Delta^7Li_{regolith\text{-}bedrock}$ = −42 ‰ and $\Delta^7Li_{porewater\text{-}bedrock}$ = −31 ‰ at 9.3 m depth; Tables 1 and 2) recorded to date (compare, e.g., with compilation in Pogge von Strandmann et al., 2020).

The exchangeable fraction has the lightest Li isotopic composition of the analyzed reservoirs, from δ^7Li = −50.7 ± 0.6‰ at the bottom of the profile to δ^7Li = −21.4 ± 0.6‰ at 5.5 m depth (Table 3; Table S2 in Supporting Information S1; Figure 1d), representing differences from the bedrock of −55‰ to −25‰. The low Li concentrations in the exchangeable fraction above this depth were insufficient for Li isotope measurements.

The leaves of the predominant tree in the forest, the Tabonuco (*Dacryodes excelsa*), have a δ^7Li of +3.4‰, similar to the bedrock and to shallow porewater (Table 1; Figure 1d).

The stream δ^7Li values (+31.9‰ and +36.6‰; Table 2; Table S2 in Supporting Information S1; Figure 1d) are within the upper range of worldwide and tropical rivers (Hindshaw et al., 2019; Pogge von Strandmann et al., 2020, and references therein), but are much higher than in the similar highly weathered, andesitic Quiock Creek of Guadeloupe (about +15‰; Clergue et al., 2015; Fries et al., 2019).

4. Discussion

4.1. Sources of Li to the Regolith

The Bisley catchment bedrock contains several minerals into which Li can substitute for Mg and Fe (chlorite, pyroxene, amphibole, epidote) or, to a lesser extent, be held in interstitial sites in quartz and plagioclase (Breiter et al., 2012; Jacamon & Larsen, 2009; Lynton et al., 2005; Zhang et al., 2021). Among these potentially Li-bearing minerals, chlorite contains six times more Mg and Fe than epidote, pyroxene or amphibole, and is the most

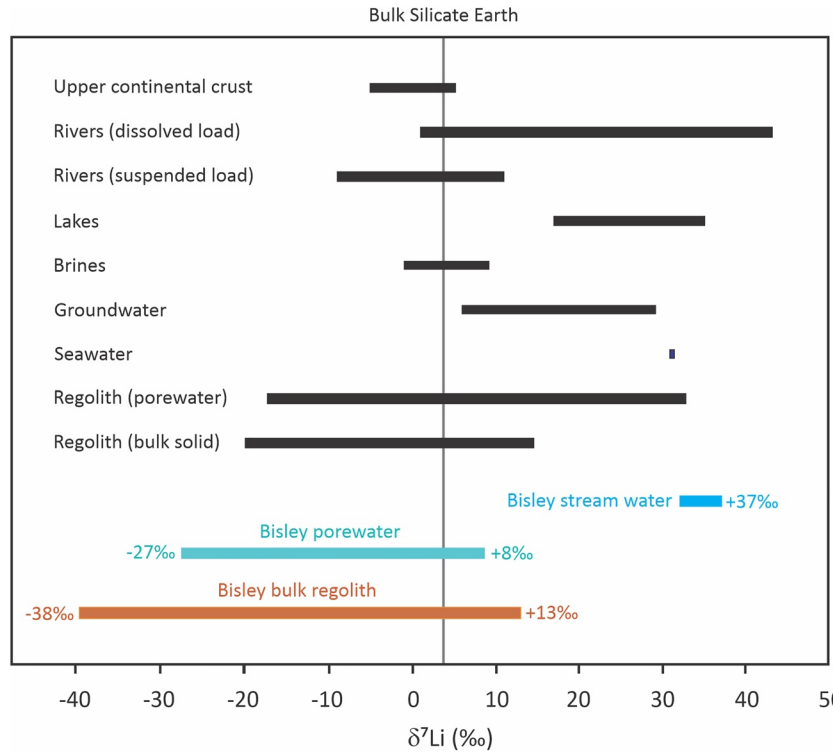

Figure 2. Comparison of the range of δ^7Li values in this work and those previously published. The range of values of river water and sediments, lakes, brines, and groundwater are from Penniston-Dorland et al. (2017) and references therein, updated to include new suspended sediment values from Millot and Négrel (2021) and Weynell et al. (2021). Previously published bulk regolith δ^7Li values range from −20‰ (Rudnick et al., 2004) to +13.9 ‰ (Ryu et al., 2014) and porewater δ^7Li values from −17‰ to +33‰ (Lemarchand et al., 2010).

abundant of the Fe-Mg minerals in the bedrock (Buss et al., 2013), making it likely to be the dominant source of Li available for weathering.

Lithium can also enter the weathering environment at the top of the profile by atmospheric inputs, as suggested by the shift in δ^7Li values (Figure 1d) and slight increase in CIA above 1.5 m depth (Figure S1a in Supporting Information S1; Table 1). However, mass-transfer calculations show that atmospheric inputs of Li are lost to weathering below 1.2 m depth, such that overall the regolith is depleted in Li as compared to the bedrock (Text S1 in Supporting Information S1).

4.2. Li Isotopic Fractionation by Weathering Processes Within the Regolith

The δ^7Li values we measured at the Bisley 1 catchment are remarkable for including the lowest ever reported regolith and porewater values, a range of δ^7Li values spanning 87‰ (Figure 2) and unexpected relationships between the regolith, porewater, and stream water (Figure 1d). We conceptualize the drivers of these Li isotopic fractionations and relationships as operating in two depth domains within the regolith profile: (a) driven by secondary mineral *precipitation* at the bedrock-regolith transition, captured from 9.3 to 8.5 m depth, and (b) driven by secondary mineral *dissolution*, from 8.5 to the surface (Figure 3). Notably, the stream draining the catchment does not seem to reflect either of these two in-regolith processes, but rather a third weathering environment (Section 4.3).

4.2.1. Secondary Mineral Precipitation at the Bedrock-Regolith Transition

As bedrock primary minerals are weathered, secondary minerals precipitate, preferentially taking up the lighter ^{6}Li and driving a progressively larger difference between bedrock and bulk regolith δ^7Li values (Clergue et al., 2015; Huh et al., 2004; Kisakürek et al., 2004; Rudnick et al., 2004; Ryu et al., 2014). At our site, this process is manifest at the bedrock-regolith transition (captured from 9.3 to 8.5 m depth) as an increase in the

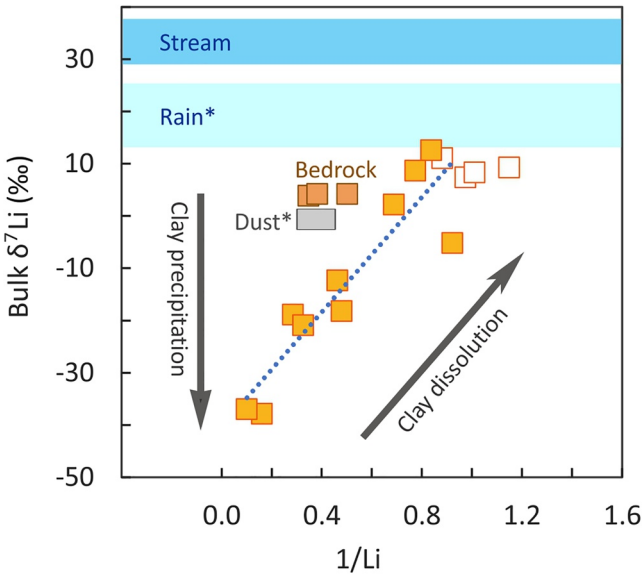

Figure 3. Bulk regolith 1/Li versus δ^7Li, showing the two different lithium isotope fractionation domains recorded in the weathering profile. (a) At the bedrock-regolith transition (9.3–8.5 m depth), clays, and other secondary minerals precipitate, with an apparent Δ^7Li of −42‰. (b) As weathering advances from the clay precipitation domain toward the surface of the profile (Figure 4a), clays re-dissolve, with an apparent Δ^7Li of +50‰. Above 1.5 m depth, the bulk regolith is also influenced by dust inputs (empty squares). The δ^7Li of the stream, rain and dust are shown for comparison (1/Li arbitrary). *Dust and rain values are from the Caribbean island of Guadeloupe (Clergue et al., 2015).

overall weathering degree (CIA = 96% at 9.3 m depth, rising to >99% at 8.2 m; Figure S2a in Supporting Information S1), a loss of most remaining primary minerals (Figure S2c and Table S1 in Supporting Information S1) and a large difference between bedrock and deep regolith δ^7Li values (Δ^7Li $_{\text{regolith-bedrock}} = -42‰$; Figure 3). However, we note that even our deepest regolith sample (collected at 9.3 m depth, the depth of auger refusal) is already highly altered (CIA = 96%; Figure S2a in Supporting Information S1), indicating that most of the chemical weathering that transforms fresh bedrock into regolith happens at a scale below the resolution of our sampling. Indeed, Moore et al. (2019) showed that weathering along deep bedrock fractures in the Bisley 1 catchment is significant: 70% of overall alteration (CIA) can be observed within 10 mm of a fracture surface and up to 90% of the fresh bedrock cations are depleted within 60 mm of fracture surfaces.

Among the Li-bearing minerals in the bedrock, only chlorite, quartz, and orthoclase remain at the bedrock-regolith transition coincident with our deepest samples (9.3–8.5 m depth; Figure S2c in Supporting Information S1), but quartz does not dissolve at the bedrock-regolith transition or along the bedrock fractures at this site (Buss et al., 2017). Therefore, the δ^7Li signature of the secondary mineral precipitation domain (Figure 3) can be expressed in a simplified form as the balance between chlorite and orthoclase dissolution and kaolinite (Kaol), illite and Fe(III)-(hydr)oxide (Fe-Ox) precipitation:

$$\text{Chlorite} + \text{Orthoclase} \rightarrow \text{Illite}(^6\text{Li}) + \text{Kaol}(^6\text{Li}) + \text{Fe}-\text{Ox}(^6\text{Li}) + {}^7\text{Li}^+_{(aq)} + \text{H}^+_{(aq)} \quad (1)$$

where, the isotope enriched in each phase is given in parentheses and other cations released during primary mineral dissolution are neglected.

The ^{7}Li-enriched porewater produced by Equation 1 is likely drained rapidly from the regolith through the highly fractured bedrock (Buss et al., 2013; Moore et al., 2019), and continually mixed with water infiltrating from the overlying regolith (infiltration rate ~5 m y^{-1}; Buss et al., 2017).

The high infiltration rate would make advection the predominant way of Li transport for most of the profile. However, at the bedrock regolith transition a sharp decrease in permeability may occur, slowing water movement such that diffusion may be a relevant Li fractionating process within the clay precipitation domain (e.g., Teng et al., 2010). Lithium isotope fractionation by diffusion is characterized by larger fractionation factors than at equilibrium (e.g., Li et al., 2021; Li & Liu, 2020; Verney-Carron et al., 2015), which could also contribute to the large apparent fractionation between the bedrock and the deepest regolith (Δ^7Li $_{\text{regolith-bedrock}} = -42‰$). Moreover, the dissolution of chlorite and orthoclase (Equation 1; Figure S2c in Supporting Information S1) increases the pH by about one unit at this depth (Buss et al., 2017), which would enhance kinetic fractionation by sorption onto clays (Li & Liu, 2020).

4.2.2. Secondary Mineral Dissolution Within the Regolith

Above the secondary mineral precipitation domain (9.3–8.5 m), δ^7Li values in bulk regolith (δ^7Li$_{\text{bulk}}$) and porewater (δ^7Li$_{\text{porewater}}$) increase toward the surface of the profile, with δ^7Li$_{\text{porewater}}$ consistently lower than δ^7Li$_{\text{bulk}}$ (Figure 1d). This relationship is the opposite of that expected from the chemical weathering of most primary silicates, by which the lighter ^{6}Li isotope usually accumulates in the solid as weathering advances, producing δ^7Li$_{\text{bulk}}$ < δ^7Li$_{\text{porewater}}$ (Pogge von Strandmann et al., 2020). Instead, the observed δ^7Li$_{\text{bulk}}$ > δ^7Li$_{\text{porewater}}$ relationship is consistent with the preferential leaching of the lighter ^{6}Li as Li is lost from the bulk regolith (Figure 4b, Figure S2b in Supporting Information S1).

The mineralogy of the regolith within this depth domain is composed entirely of clays (~77 wt. %), quartz (~18 wt. %) and Fe(III)-(hydr)oxides (~5 wt. %; Figure S2c and Table S1 in Supporting Information S1; Buss et al., 2017), although with some atmospheric input superimposed in the upper 1.5 m (Figure S2b and Text S1

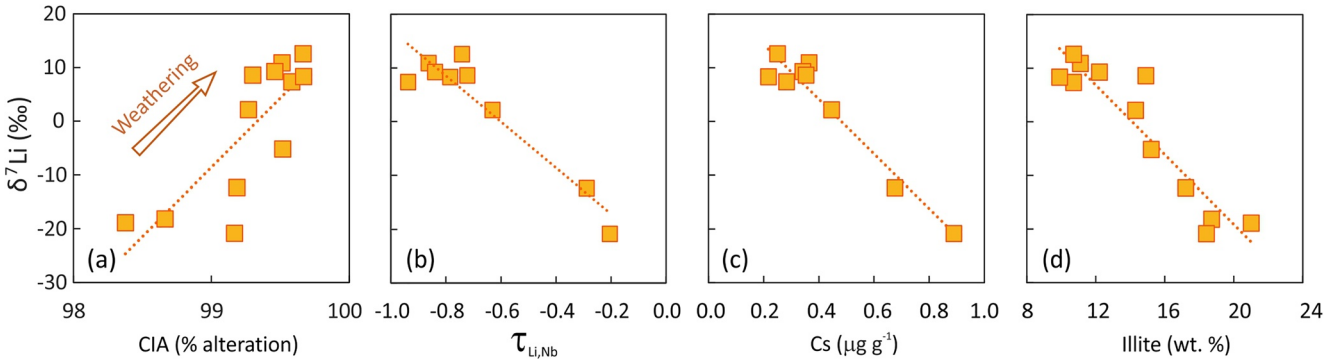

Figure 4. Above the clay precipitation domain (>8.5 m depth), bulk solid δ^7Li is positively correlated with (a) weathering degree ($r^2 = 0.63$), approximated by the Chemical Index of Alteration (Equation S1 in Supporting Information S1). δ^7Li is also negatively correlated with (b) the mass transfer index $\tau_{Li,Nb}$ (Equation S2 in Supporting Information S1; $r^2 = 0.87$); (c) Cs ($r^2 = 0.93$), a proxy for total clay abundance (including amorphous phases not detectable by XRD); and with (d) illite content ($r^2 = 0.85$), indicating clay dissolution is the main process driving Li isotope fractionation in this domain. We found no correlation between δ^7Li and the rest of the regolith minerals (kaolinite, quartz or Fe-oxides; not shown).

in Supporting Information S1). These minerals are relatively stable at Earth's surface conditions, but under the intense weathering of the humid tropics, clays and even quartz start to break down (Buss et al., 2017; Schulz & White, 1999). Another common process in tropical soils is that short-range-order Fe(III)-(hydr)oxides and Al-oxides increase in crystallinity (e.g., Chadwick & Chorover, 2001; Chorover et al., 2004), expelling impurities such as Li. Among these secondary mineral-mediated reactions, however, clay dissolution is most likely driving the Li isotopic variability above 8.5 m depth (Figures 4a–4d), as suggested by the inverse correlation between bulk δ^7Li and Cs (Figure 4c), a proxy for overall clay abundance (including the amorphous phases that are common in tropical soils and hard to detect by XRD) because of its high affinity for clays (Sawhiney, 1972).

More specifically, illite is the only identified mineral (Figure S2c in Supporting Information S1; Buss et al., 2017) to show a clear correlation with δ^7Li (Figure 4d), indicating that illite dissolution may be the predominant process behind the wide Li isotope variation within this depth interval (Figure 3). Therefore, within this domain of clay dissolution (Figure 3), we suggest the ^{6}Li-enriched illite that initially precipitated at the bedrock-regolith transition (Equation 1) dissolves, producing porewater enriched in ^{6}Li via Equation 2 below (with the isotope enriched in each phase given in parentheses).

$$\text{Illite}(^6\text{Li}) \rightarrow {}^6\text{Li}^+_{(aq)} + \text{SiO}_{2(aq)} + \text{other ions in solution} \quad (2)$$

The isotopically light porewaters generated in this clay dissolution domain (Equation 2) move downwards through the regolith and may also be re-incorporated into the clays that are precipitating in the bedrock-regolith transition (Equation 1; Figure 3), possibly including an initial diffusion step (Li & Liu, 2020). This "^{6}Li-recycling" mechanism would increase the size of the apparent isotopic fractionation during clay precipitation in the bedrock-regolith transition zone and is consistent with the ca. 150% enrichment in Li observed there relative to the bedrock ($\tau_{Li,Nb} \approx 1.48$; Figure S2b in Supporting Information S1, Figure 1d; Table 1).

The exchangeable fraction represents only between 0.1% and 0.3% of the bulk solid Li in this profile (Figures 1a and 1b; Tables 1 and 2), and thus exerts little influence on the overall δ^7Li signature of the regolith, but it nevertheless constitutes a distinct Li pool that is isotopically lighter than the structural Li pool by up to 11‰ (Figure 1d; Tables 1 and 3). In contrast, experimental studies have shown that Li in clays is held in two isotopically distinct pools (exchangeable and structural), but with structurally bound Li favoring the lighter ^{6}Li and exchangeable Li taken up with little isotope fractionation (Hindshaw et al., 2019; Pistiner & Henderson, 2003; Pogge von Strandmann, Fraser, et al., 2019; Vigier et al., 2008). This could indicate that fractionation of Li during outer-sphere adsorption is larger for our mineral assemblage than has been observed for the pure minerals used in experiments. Alternatively, this lighter exchangeable fraction could reflect continuous exchange with isotopically lighter Li leached from the upper parts of the profile or kinetic isotope effects at the initial step of sorption onto clays (Li & Liu, 2020).

4.3. Li Isotopic Fractionation Below the Regolith

Using the Cl balance method to subtract rain inputs from the Li concentration in stream water, we estimate that roughly 70% of Li in the Bisley 1 stream comes from weathering sources during low flow (Text S2 in Supporting Information S1). However, we cannot link this weathering source of Li to either of the two domains we identified within the regolith (Section 4.1), because porewater has substantially lower δ^7Li values (−26.7 to +7.9‰) than the streamwater (+36‰; Figures 1d, 2, and 3). Instead, the extremely low δ^7Li in all measured fractions of the deep regolith relative to the bulk bedrock (Figure 1d) indicates that a component of bedrock-derived ^{7}Li is missing. This component could be lost from bedrock weathering along mm-scale interfaces in fractures below the zone sampled by the auger which, as mentioned in Section 4.2.1, constitutes the majority of weathering in this catchment. In this deeper weathering environment, dissolved ^{7}Li is likely flushed from the weathering interfaces rapidly, which could lead to the high δ^7Li measured in the stream water, while the dissolved ^{6}Li would be largely retained on exchange sites and neo-formed clays. Therefore, weathering along bedrock fractures is likely the main source of Li to the stream, consistent with previous studies that found a source of solutes deeper than 9.3 m is necessary to close the isotopic (Chapela Lara et al., 2017; Yi-Balan et al., 2014) and elemental (Schellekens et al., 2004) budgets of the Bisley catchments.

4.4. Implications for the δ^7Li Signature of Highly Weathered Catchments

The current understanding of Li isotope systematics is that as weathering increases from low to intermediate intensity, secondary mineral precipitation drives the δ^7Li of stream waters toward values higher than the bedrock, whereas with further weathering waters increasingly reflect the low δ^7Li of the weathered regolith and re-approach bedrock values (Dellinger et al., 2014; Huh et al., 2001; Misra & Froelich, 2012). This conceptual model would predict low, near-bedrock δ^7Li values for the stream in the high weathering intensity Bisley 1 catchment, which instead has much higher values that are more consistent with an intermediate weathering regime. However, we note that these broad models about δ^7Li behavior are hampered by the very limited number of field studies in highly weathered catchments published to date (Clergue et al., 2015; Dellinger et al., 2014, 2015; Fries et al., 2019; Huh et al., 2001).

Our study and those in the Caribbean island of Guadeloupe (Clergue et al., 2015; Fries et al., 2019) are particularly relevant to fill this gap because they represent extreme examples of supply limited weathering regimes, where the Li isotopic composition of both the solid and the liquid products of weathering have been measured. Both of these catchments are relatively small (Quiock Creek ~8 ha; Bisley 1 ~7 ha), underlain by andesitic bedrock and covered by deep (>10 m) highly weathered regolith (CIA >99%) under a wet tropical climate. However, despite these similarities, the streams at both sites have very different δ^7Li values, which may indicate that dissolved Li is sourced from different weathering processes, likely occurring at different zones of the catchment. In Guadeloupe, the stream δ^7Li values (~+9.3 ‰) are similar to porewater and to the local bedrock (δ^7Li = +5.3‰), consistent with the Dellinger et al. (2015) model and suggesting a direct connection between weathering processes in the regolith and the composition of the stream (e.g., 52%–73% of Li comes from regolith porewater during low flow; Fries et al., 2019). In contrast, at our site in Puerto Rico, the extremely low δ^7Li values of porewater are not reflected in the composition of the stream at low flow (~+36‰; Figure 1d), indicating that the stream water δ^7Li signature is not directly derived from regolith porewater.

The reason for the apparent decoupling between δ^7Li in porewater and stream water at our site (Figure 1d), in contrast to what was observed in Guadeloupe, cannot be established definitively without a dedicated mineralogical and hydrological study, perhaps incorporating reactive transport modeling (Golla et al., 2021). However, we suggest that this different behavior may stem from the different relationship between the water table and the sampled profile depths at the two sites. In Guadeloupe, the water table is reached within the sampled 14 m of regolith profile (Fries et al., 2019) and thus its chemistry reflects weathering reactions within the regolith. In Bisley, the groundwater level remains below the 10 m of the regolith profile even during large storm events, reflecting reactions along deeper water pathways in fractured rock, where relatively Li-rich primary minerals are still being altered to secondary minerals. In other words, although secondary mineral precipitation-dissolution reactions appear to set the δ^7Li signatures in most of our regolith profile, these regolith signals are not transmitted to the stream water draining the catchment because of the hydrological setting.

Our data thus suggest that, although the δ^7Li signature of dissolved weathering products may reliably predict weathering intensity (i.e., degree of regolith weathering) in most catchments (Dellinger et al., 2015), in higher weathering intensity settings the relationship may not always hold. Specifically, we show that in extreme weathering regimes, the apparent weathering intensity of the catchment's regolith and porewater can be entirely disconnected from the weathering intensity of the key zone where the majority of weathering-derived Li is produced. In such environments, the liquid products of weathering can keep evolving toward isotopically lighter values as weathering advances, without the streams becoming isotopically lighter.

The decoupling between the regolith and the stream water's δ^7Li values has implications for interpreting the δ^7Li of past seawater, where it is commonly assumed that intensely weathered continents (such as those of the early Cenozoic) should automatically be reflected in isotopically light riverine fluxes of Li (e.g., Misra & Froelich, 2012), something our data caution against. The threshold for this decoupled behavior might be controlled by the limit in the supply of fresh minerals, in turn modulated by erosion rates in larger catchments as proposed by Dellinger et al. (2015). However, our work demonstrates that even in catchments of comparable size, erosion and weathering rates (cf. Guadeloupe and Bisley), markedly different δ^7Li values might arise, reflecting the local hydrological and mineralogical properties of the catchment rather than weathering degree per se.

5. Conclusions

At the site where the highest silicate weathering rates on Earth have been reported (Bisley 1, Puerto Rico), we found the lowest δ^7Li values measured to date in porewater (−27‰), bulk regolith (−38‰) and exchangeable Li (−50‰). We also found unusual relationships between the Li pools in the regolith, with lower δ^7Li values in the exchangeable fraction than in porewater or bulk solid. We interpret these extreme δ^7Li values and the relationships between Li pools as the result of two distinct weathering processes within the regolith, both driven by secondary minerals: (a) clay precipitation at the bedrock-regolith transition, with a preference for the lighter ^{6}Li isotope possibly enhanced by diffusion and (b) clay dissolution as weathering advances further up the profile. During this second process, ^{6}Li is leached down and likely incorporated again into the clays that are forming at the bedrock-regolith transition (process 1, above), likely increasing the apparent bedrock-regolith fractionation at the base of the profile. Surprisingly, we also found that these two weathering processes within the regolith are not reflected in the δ^7Li signature of the local stream, which instead shows high δ^7Li values typical of medium-intensity weathering. This result indicates that the stream Li isotopic signature is likely to be controlled by clay precipitation in bedrock fractures at greater depth than the ~10 m deep weathering profile we sampled, thus reflecting the local hydrology and deep water-rock interactions rather than the overall weathering intensity in the catchment.

In a broader context, our results and those from a comparable highly weathered andesitic site in the Caribbean, expand our current understanding of Li isotopic systematics by demonstrating that the weathering intensity of the regolith covering a catchment can be disconnected from the isotopic signature of its stream, even under very similar bedrock and climate conditions. In these highly leached tropical environments, the liquid products of weathering can evolve toward extremely low δ^7Li values as weathering advances, without the stream necessarily becoming isotopically lighter, highlighting the importance of further research in constraining the controls over Li isotope signatures in highly weathered settings.

Conflict of Interest

The authors declare no conflict of interest relevant to this study.

Data Availability Statement

All the data used for this work are provided within the manuscript and in the Supporting Information S1. In addition, the data generated in this paper are available in Hydroshare.org at https://doi.org/10.4211/hs.28acde53dc5549f4a6e5d820364dd216 (Chapela Lara et al., 2022). The ancillary data contained in the Supporting Information S1 are also available in Hydroshare.org (Buss et al., 2021; Chapela Lara et al., 2021) or in the Environmental Data Initiative at https://portal.edirepository.org (McDowell et al., 2021a, 2021b).

Acknowledgments
We are grateful to Friedhelm von Blanckenburg for useful conversations, Daniel A. Frick for analytical assistance, HELGES laboratory staff (especially Jutta Schlegel and Josefine Holtz) for their help in processing and measuring samples, Jody Potter (UNH Water Quality laboratory) for sample management and Miguel Leon for guidance in making our data publicly available. We also appreciate the editorial handling of Mikael Attal and Lixin Jin and the constructive comments of three anonymous reviewers, which greatly improved our manuscript. This work was funded by the NSF Luquillo Critical Zone Observatory grants EAR-0722476 and EAR-1331841 to WHM and a Research Fellowship from the Alexander von Humboldt Foundation to MCL. Open access funding enabled and organized by Projekt DEAL.

References

Breiter, K., Svojtka, M., Ackerman, L., & Švecová, K. (2012). Trace element composition of quartz from the Variscan Altenberg–Teplice caldera (Krušné hory/Erzgebirge Mts, Czech Republic/Germany): Insights into the volcano-plutonic complex evolution. *Chemical Geology*, *326–327*, 36–50. https://doi.org/10.1016/j.chemgeo.2012.07.028

Buss, H. L., Brantley, S. L., Scatena, F. N., Bazilievskaya, E. A., Blum, A., & Schulz, M. (2013). Probing the deep critical zone beneath the Luquillo Experimental Forest, Puerto Rico. *Earth Surface Processes and Landforms*, *38*(10), 1170–1186. https://doi.org/10.1002/esp.3409

Buss, H. L., Chapela Lara, M., Moore, O. W., Kurtz, A. C., Schulz, M. S., & White, A. F. (2017). Lithological influences on contemporary and long-term regolith weathering at the Luquillo Critical Zone Observatory. *Geochimica et Cosmochimica Acta*, *196*, 224–251. https://doi.org/10.1016/j.gca.2016.09.038

Buss, H. L., Kurtz, A. C., Chapela Lara, M., White, A. F., Schulz, M. S., & Moore, O. W. (2021). *LCZO-Geology, Regolith Survey, Lithological influences on contemporary and long-term regolith weathering at the Luquillo Critical Zone Observatory-Bisley and Icacos (2015–2017)*. HydroShare. Retrieved from http://www.hydroshare.org/resource/70d6eeb63e154f8197467e1f7c91f55b

Chadwick, O. A., & Chorover, J. (2001). The chemistry of pedogenic thresholds. *Geoderma*, *100*, 321–353. https://doi.org/10.1016/s0016-7061(01)00027-1

Chapela Lara, M., Buss, H. L., Henehan, M. J., Schuessler, J. A., & McDowell, W. H. (2022). *LCZO-Lithium isotopic composition and ancillary geochemical data for regolith profile B1S1 (Bisley 1, ridgetop site)*. HydroShare. Retrieved from http://www.hydroshare.org/resource/28acde53dc5549f4a6e5d820364dd216

Chapela Lara, M., Buss, H. L., & Pett-Ridge, J. C. (2018). The effects of lithology on trace element and REE behavior during tropical weathering. *Chemical Geology*, *500*, 88–102. https://doi.org/10.1016/j.chemgeo.2018.09.024

Chapela Lara, M., Buss, H. L., & Pett-Ridge, J. C. (2021). *LCZO-Geology, Regolith Survey, trace and rare earth elements-Bisley and Icacos (2017)*. HydroShare. Retrieved from http://www.hydroshare.org/resource/c646475a6c224f5d838f450ba0947f01

Chapela Lara, M., Buss, H. L., Pogge von Strandmann, P. A. E., Schuessler, J. A., & Moore, O. W. (2017). The influence of critical zone processes on the Mg isotope budget in a tropical, highly weathered andesitic catchment. *Geochimica et Cosmochimica Acta*, *202*, 77–100. https://doi.org/10.1016/j.gca.2016.12.032

Choi, M. S., Ryu, J.-S., Park, H. Y., Lee, K.-S., Kil, Y., & Shin, H. S. (2013). Precise determination of the lithium isotope ratio in geological samples using MC-ICP-MS with cool plasma. *Journal of Analytical Atomic Spectrometry*, *28*(4), 505–509. https://doi.org/10.1039/C2JA30293D

Chorover, J., Amistadi, M. K., & Chadwick, O. A. (2004). Surface charge evolution of mineral-organic complexes during pedogenesis in Hawaiian basalt. *Geochimica et Cosmochimica Acta*, *68*(23), 4859–4876. https://doi.org/10.1016/j.gca.2004.06.005

Clergue, C., Dellinger, M., Buss, H. L., Gaillardet, J., Benedetti, M. F., & Dessert, C. (2015). Influence of atmospheric deposits and secondary minerals on Li isotopes budget in a highly weathered catchment, Guadeloupe (Lesser Antilles). *Chemical Geology*, *414*, 28–41. https://doi.org/10.1016/j.chemgeo.2015.08.015

Dellinger, M., Gaillardet, J., Bouchez, J., Calmels, D., Galy, V., Hilton, R. G., et al. (2014). Lithium isotopes in large rivers reveal the cannibalistic nature of modern continental weathering and erosion. *Earth and Planetary Science Letters*, *401*, 359–372. https://doi.org/10.1016/j.epsl.2014.05.061

Dellinger, M., Gaillardet, J., Bouchez, J., Calmels, D., Louvat, P., Dosseto, A., et al. (2015). Riverine Li isotope fractionation in the Amazon River basin controlled by the weathering regimes. *Geochimica et Cosmochimica Acta*, *164*, 71–93. https://doi.org/10.1016/j.gca.2015.04.042

Dosseto, A., Buss, H. L., & Suresh, P. O. (2012). Rapid regolith formation over volcanic bedrock and implications for landscape evolution. *Earth and Planetary Science Letters*, *337–338*, 47–55. https://doi.org/10.1016/j.epsl.2012.05.008

Fries, D. M., James, R. H., Dessert, C., Bouchez, J., Beaumais, A., & Pearce, C. R. (2019). The response of Li and Mg isotopes to rain events in a highly-weathered catchment. *Chemical Geology*, *519*, 68–82. https://doi.org/10.1016/j.chemgeo.2019.04.023

Gioda, A., Mayol-Bracero, O. L., Scatena, F. N., Weathers, K. C., Mateus, V. L., & McDowell, W. H. (2013). Chemical constituents in clouds and rainwater in the Puerto Rican rainforest: Potential sources and seasonal drivers. *Atmospheric Environment*, *68*, 208–220. https://doi.org/10.1016/j.atmosenv.2012.11.017

Golla, J. K., Kuessner, M. L., Henehan, M. J., Bouchez, J., Rempe, D. M., & Druhan, J. L. (2021). The evolution of lithium isotope signatures in fluids draining actively weathering hillslopes. *Earth and Planetary Science Letters*, *567*, 116988. https://doi.org/10.1016/j.epsl.2021.116988

Henchiri, S., Clergue, C., Dellinger, M., Gaillardet, J., Louvat, P., & Bouchez, J. (2014). The influence of hydrothermal activity on the Li isotopic signature of rivers draining volcanic areas. *Procedia Earth and Planetary Science*, *10*, 223–230. https://doi.org/10.1016/j.proeps.2014.08.026

Hindshaw, R. S., Tosca, R., Goût, T. L., Farnan, I., Tosca, N. J., & Tipper, E. T. (2019). Experimental constraints on Li isotope fractionation during clay formation. *Geochimica et Cosmochimica Acta*, *250*, 219–237https://doi.org/10.1016/j.gca.2019.02.015

Huh, Y., Chan, L.-H., & Chadwick, O. A. (2004). Behavior of lithium and its isotopes during weathering of Hawaiian basalt. *Geochemistry, Geophysics, Geosystems*, *5*, Q09002. https://doi.org/10.1029/2004gc000729

Huh, Y., Chan, L.-H., & Edmond, J. M. (2001). Lithium isotopes as a probe of weathering processes: Orinoco River. *Earth and Planetary Science Letters*, *194*(1), 189–199. https://doi.org/10.1016/s0012-821x(01)00523-4

Huh, Y., Chan, L.-H., Zhang, L., & Edmond, J. M. (1998). Lithium and its isotopes in major world rivers: Implications for weathering and the oceanic budget. *Geochimica et Cosmochimica Acta*, *62*, 2039–2051. https://doi.org/10.1016/s0016-7037(98)00126-4

Jacamon, F., & Larsen, R. B. (2009). Trace element evolution of quartz in the charnockitic Kleivan granite, SW-Norway: The Ge/Ti ratio of quartz as an index of igneous differentiation. *Lithos*, *107*(3), 281–291. https://doi.org/10.1016/j.lithos.2008.10.016

Kisakürek, B., James, R. H., & Harris, N. B. W. (2005). Li and δ7Li in Himalayan rivers: Proxies for silicate weathering? *Earth and Planetary Science Letters*, *237*(3), 387–401. https://doi.org/10.1016/j.epsl.2005.07.019

Kisakürek, B., Widdowson, M., & James, R. H. (2004). Behaviour of Li isotopes during continental weathering: The Bidar laterite profile, India. *Chemical Geology*, *212*(1), 27–44. https://doi.org/10.1016/j.chemgeo.2004.08.027

Kuessner, M. L., Gourgiotis, A., Manhès, G., Bouchez, J., Zhang, X., & Gaillardet, J. (2020). Automated analyte separation by ion Chromatography using a Cobot applied to geological reference materials for Li isotope composition. *Geostandards and Geoanalytical Research*, *44*(1), 57–67. https://doi.org/10.1111/ggr.12295

Lemarchand, E., Chabaux, F., Vigier, N., Millot, R., & Pierret, M. C. (2010). Lithium isotope systematics in a forested granitic catchment (Strengbach, Vosges Mountains, France). *Geochimica et Cosmochimica Acta*, *74*, 4612–4628. https://doi.org/10.1016/j.gca.2010.04.057

Li, W., & Liu, X.-M. (2020). Experimental investigation of lithium isotope fractionation during kaolinite adsorption: Implications for chemical weathering. *Geochimica et Cosmochimica Acta*, *284*, 156–172. https://doi.org/10.1016/j.gca.2020.06.025

Li, W., Liu, X.-M., Wang, K., & Koefoed, P. (2021). Lithium and potassium isotope fractionation during silicate rock dissolution: An experimental approach. *Chemical Geology*, *568*, 120142. https://doi.org/10.1016/j.chemgeo.2021.120142

Liu, X.-M., Rudnick, R. L., McDonough, W. F., & Cummings, M. L. (2013). Influence of chemical weathering on the composition of the continental crust: Insights from Li and Nd isotopes in bauxite profiles developed on Columbia River Basalts. *Geochimica et Cosmochimica Acta*, *115*, 73–91. https://doi.org/10.1016/j.gca.2013.03.043

Lynton, S. J., Walker, R. J., & Candela, P. A. (2005). Lithium isotopes in the system Qz-Ms-fluid:An experimental study. *Geochimica et Cosmochimica Acta*, *69*(13), 3337–3347. https://doi.org/10.1016/j.gca.2005.02.009

McClintock, M. A., Brocard, G., Willenbring, J., Tamayo, C., Porder, S., & Pett-Ridge, J. C. (2015). Spatial variability of African dust in soils in a montane tropical landscape in Puerto Rico. *Chemical Geology*, *412*, 69–81. https://doi.org/10.1016/j.chemgeo.2015.06.032

McDowell, W. (2021a). *Chemistry of rainfall and throughfall from El Verde and Bisley ver 2110857*. Environmental Data Initiative. https://doi.org/10.6073/pasta/636e65184c885a603fef603cf361dc11 (Accessed 2021-11-17).

McDowell, W. (2021b). *Chemistry of stream water from the Luquillo Mountains ver 4923056*. Environmental Data Initiative. https://doi.org/10.6073/pasta/0a09f5aa2e6f11451553c92b102279a6 (Accessed 2021-11-17).

McDowell, W. H., Leon, M. C., Shattuck, M. D., Potter, J. D., Heartsill-Scalley, T., González, G., et al. (2021c). Luquillo experimental forest: Catchment science in the montane tropics. *Hydrological processes*, *35*, e14146. https://doi.org/10.1002/hyp.14146

Millot, R., & Négrel, P. (2021). Lithium isotopes in the Loire River Basin (France): Hydrogeochemical characterizations at two complementary scales. *Applied Geochemistry*, *125*, 104831. https://doi.org/10.1016/j.apgeochem.2020.104831

Millot, R., Vigier, N., & Gaillardet, J. (2010). Behaviour of lithium and its isotopes during weathering in the Mackenzie Basin, Canada. *Geochimica et Cosmochimica Acta*, *74*(14), 3897–3912. https://doi.org/10.1016/j.gca.2010.04.025

Misra, S., & Froelich, P. N. (2012). Lithium isotope history of Cenozoic Seawater: Changes in silicate weathering and reverse weathering. *Science*, *335*(6070), 818–823. https://doi.org/10.1126/science.1214697

Moore, O. W., Buss, H. L., & Dosseto, A. (2019). Incipient chemical weathering at bedrock fracture interfaces in a tropical critical zone system, Puerto Rico. *Geochimica et Cosmochimica Acta*, *252*, 61–87. https://doi.org/10.1016/j.gca.2019.02.028

Murphy, S. F., & Stallard, R. F. (2012). Hydrology and climate of four watersheds in eastern Puerto Rico. In S. F. Murphy, & R. F. Stallard (Eds.), *Water quality and landscape processes of four watersheds in eastern Puerto Rico* (Vol. 1789, pp. 47–83).

Penniston-Dorland, S., Liu, X.-M., & Rudnick, R. L. (2017). Lithium isotope geochemistry. *Reviews in Mineralogy and Geochemistry*, *82*(1), 165. https://doi.org/10.2138/rmg.2017.82.6

Pett-Ridge, J. (2009). Contributions of dust to phosphorus cycling in tropical forests of the Luquillo Mountains, Puerto Rico. *Biogeochemistry*, *94*(1), 63–80. https://doi.org/10.1007/s10533-009-9308-x

Pistiner, J. S., & Henderson, G. M. (2003). Lithium-isotope fractionation during continental weathering processes. *Earth and Planetary Science Letters*, *214*(1–2), 327–339. https://doi.org/10.1016/s0012-821x(03)00348-0

Pogge von Strandmann, P. A. E., Burton, K. W., James, R. H., van Calsteren, P., Gíslason, S. R., & Mokadem, F. (2006). Riverine behaviour of uranium and lithium isotopes in an actively glaciated basaltic terrain. *Earth and Planetary Science Letters*, *251*(1–2), 134–147. https://doi.org/10.1016/j.epsl.2006.09.001

Pogge von Strandmann, P. A. E., Fraser, W. T., Hammond, S. J., Tarbuck, G., Wood, I. G., Oelkers, E. H., & Murphy, M. J. (2019). Experimental determination of Li isotope behaviour during basalt weathering. *Chemical Geology*, *517*, 34–43. https://doi.org/10.1016/j.chemgeo.2019.04.020

Pogge von Strandmann, P. A. E., Kasemann, S. A., & Wimpenny, J. B. (2020). Lithium and lithium isotopes in Earth's surface cycles. *Elements*, *16*(4), 253–258. https://doi.org/10.2138/gselements.16.4.253

Pogge von Strandmann, P. A. E., Opfergelt, S., Lai, Y.-J., Sigfusson, B. R., Gislason, S., & Burton, K. W. (2012). Lithium, magnesium and silicon isotope behaviour accompanying weathering in a basaltic soil and pore water profile in Iceland. *Earth and Planetary Science Letters*, *339–340*, 11–23. https://doi.org/10.1016/j.epsl.2012.05.035

Pogge von Strandmann, P. A. E., Schmidt, D. N., Planavsky, N. J., Wei, G., Todd, C. L., & Baumann, K.-H. (2019). Assessing bulk carbonates as archives for seawater Li isotope ratios. *Chemical Geology*, *530*, 119338. https://doi.org/10.1016/j.chemgeo.2019.119338

Rudnick, R. L., Tomascak, P. B., Njo, H. B., & Gardner, L. R. (2004). Extreme lithium isotopic fractionation during continental weathering revealed in saprolites from South Carolina. *Chemical Geology*, *212*(1–2), 45–57. https://doi.org/10.1016/j.chemgeo.2004.08.008

Ryu, J.-S., Vigier, N., Lee, S.-W., Lee, K.-S., & Chadwick, O. A. (2014). Variation of lithium isotope geochemistry during basalt weathering and secondary mineral transformations in Hawaii. *Geochimica et Cosmochimica Acta*, *145*, 103–115. https://doi.org/10.1016/j.gca.2014.08.030

Sawhiney, B. (1972). Selective sorption and fixation of cations by clay minerals: A review. *Clays and Clay Minerals*, *29*, 93–100.

Schellekens, J., Scatena, F. N., Bruijnzeel, L. A., van Dijk, A. I. J. M., Groen, M. M. A., & van Hogezand, R. J. P. (2004). Stormflow generation in a small rainforest catchment in the Luquillo Experimental Forest, Puerto Rico. *Hydrological Processes*, *18*, 505–530. https://doi.org/10.1002/hyp.1335

Schuessler, J. A., von Blanckenburg, F., Bouchez, J., Uhlig, D., & Hewawasam, T. (2018). Nutrient cycling in a tropical montane rainforest under a supply-limited weathering regime traced by elemental mass balances and Mg stable isotopes. *Chemical Geology*. *497*, 74–87. https://doi.org/10.1016/j.chemgeo.2018.08.024

Schulz, M. S., & White, A. F. (1999). Chemical weathering in a tropical watershed, Luquillo Mountains, Puerto Rico; III. Quartz dissolution rates. *Geochimica et Cosmochimica Acta*, *63*(3–4), 337–350. https://doi.org/10.1016/s0016-7037(99)00056-3

Teng, F. Z., Li, W. Y., Rudnick, R. L., & Gardner, L. R. (2010). Contrasting lithium and magnesium isotope fractionation during continental weathering. *Earth and Planetary Science Letters*, *300*, 63–71. https://doi.org/10.1016/j.epsl.2010.09.036

Verney-Carron, A., Vigier, N., & Millot, R. (2011). Experimental determination of the role of diffusion on Li isotope fractionation during basaltic glass weathering. *Geochimica et Cosmochimica Acta*, *75*, 3452–3468. https://doi.org/10.1016/j.gca.2011.03.019

Verney-Carron, A., Vigier, N., Millot, R., & Hardarson, B. S. (2015). Lithium isotopes in hydrothermally altered basalts from Hengill (SW Iceland). *Earth and Planetary Science Letters*, *411*, 62–71. https://doi.org/10.1016/j.epsl.2014.11.047

Vigier, N., Decarreau, A., Millot, R., Carignan, J., Petit, S., & France-Lanord, C. (2008). Quantifying Li isotope fractionation during smectite formation and implications for the Li cycle. *Geochimica et Cosmochimica Acta*, *72*, 780–792. https://doi.org/10.1016/j.gca.2007.11.011

Vigier, N., Gislason, S. R., Burton, K. W., Millot, R., & Mokadem, F. (2009). The relationship between riverine lithium isotope composition and silicate weathering rates in Iceland. *Earth and Planetary Science Letters*, *287*(3–4), 434–441. https://doi.org/10.1016/j.epsl.2009.08.026

Weynell, M., Wiechert, U., & Schuessler, J. A. (2017). Lithium isotopes and implications on chemical weathering in the catchment of Lake Donggi Cona, northeastern Tibetan Plateau. *Geochimica et Cosmochimica Acta*, *213*, 155–177. https://doi.org/10.1016/j.gca.2017.06.026

Weynell, M., Wiechert, U., & Schuessler, J. A. (2021). Lithium isotope signatures of weathering in the hyper-arid climate of the western Tibetan Plateau. *Geochimica et Cosmochimica Acta*, *293*, 205–223. https://doi.org/10.1016/j.gca.2020.10.021

Wimpenny, J., Colla, C. A., Yu, P., Yin, Q.-Z., Rustad, J. R., & Casey, W. H. (2015). Lithium isotope fractionation during uptake by gibbsite. *Geochimica et Cosmochimica Acta*, *168*, 133–150. https://doi.org/10.1016/j.gca.2015.07.011

Yi-Balan, S. A., Amundson, R., & Buss, H. L. (2014). Decoupling of sulfur and nitrogen cycling due to biotic processes in a tropical rainforest. *Geochimica et Cosmochimica Acta*, *142*, 411–428. https://doi.org/10.1016/j.gca.2014.05.049

Zhang, J.-W., Zhao, Z.-Q., Li, X.-D., Yan, Y.-N., Lang, Y.-C., Ding, H., et al. (2021). Extremely enrichment of 7Li in highly weathered saprolites developed on granite from Huizhou, southern China. *Applied Geochemistry*, *125*, 104825. https://doi.org/10.1016/j.apgeochem.2020.104825

References From the Supporting Information

Brimhall, G. H., & Dietrich, W. E. (1987). Constitutive mass balance relations between chemical composition, volume, density, porosity, and strain in metasomatic hydrochemical systems: Results on weathering and pedogenesis. *Geochimica et Cosmochimica Acta*, *51*, 567–587. https://doi.org/10.1016/0016-7037(87)90070-6

Pett-Ridge, J. C., Monastra, V. M., Derry, L. A., & Chadwick, O. A. (2007). Importance of atmospheric inputs and Fe-oxides in controlling soil uranium budgets and behavior along a Hawaiian chronosequence. *Chemical Geology*, *244*(3–4), 691–707. https://doi.org/10.1016/j.chemgeo.2007.07.016

Nesbitt, H. W., & Young, G. M. (1982). Early Proterozoic climates and plate motions inferred from major element chemistry of lutites. *Nature*, *199*, 715–717. https://doi.org/10.1038/299715a0